



VICTORIA UNIVERSITY
MELBOURNE AUSTRALIA

Industrial water reclamation using polymeric membranes – case studies involving a car manufacturer and a beverage producer

This is the Accepted version of the following publication

Agana, Bernard, Reeve, Darrell and Orbell, John (2013) Industrial water reclamation using polymeric membranes – case studies involving a car manufacturer and a beverage producer. *Journal of Water Reuse and Desalination*, 3 (4). pp. 357-372. ISSN 2220-1319

The publisher's official version can be found at
<http://www.iwaponline.com/jwrd/003/jwrd0030357.htm>
Note that access to this version may require subscription.

Downloaded from VU Research Repository <https://vuir.vu.edu.au/24447/>

Industrial water reclamation using polymeric membranes –case studies involving a car manufacturer and a beverage producer

Bernard A. Agana¹, Darrell Reeve² and John D. Orbell^{1,2*}

School of Engineering and Science¹ and Institute for Sustainability and Innovation²,
Victoria University, PO Box 14428, Melbourne, Victoria 8001, Australia

Tel. +613 9919 8066; email: John.Orbell@vu.edu.au

ABSTRACT

This study presents the evaluation of different polymeric membranes on wastewater generated by two contrasting manufacturers. Specifically, ultrafiltration (UF) membranes were evaluated for wastewater pretreatment use while nanofiltration (NF) and reverse osmosis (RO) membranes were evaluated for wastewater reclamation use. Results show that both the ultrafiltration membranes used were not suitable for pretreatment of the oily wastewater stream due to presence of suspended cathodic electrodeposition (CED) paint particles. The CED paint particles rapidly deposit on the membrane surface resulting in severe fouling and very low permeate fluxes. With respect to the metals and beverage wastewater streams, the polyvinylidene-difluoride (PVDF) UF membrane was shown to be more suitable for pretreatment than the polyacrylonitrile (PAN) UF membrane. The PVDF-UF membrane had relatively lower flux decline rates, higher turbidity and higher TOC reduction rates. Meanwhile, the low-pressure RO membrane proved to be suitable for wastewater reclamation of the oily and beverage wastewater streams – showing low flux decline rates, high conductivity and high COD reduction rates. In terms of reclaiming the metals wastewater stream, the NF membrane proved more suitable than the low-pressure RO membrane. The NF membrane had relatively higher permeate fluxes and metals rejection rates compared to the RO membrane.

Key words Crossflow velocity, Nanofiltration, Polymeric membrane, Reverse osmosis, Transmembrane pressure, Ultrafiltration

* Corresponding author

INTRODUCTION

A number of researchers have shown that certain types of membrane can be employed for treating the various wastewaters generated during car manufacturing and beverage production. For example, it was shown in our previous work (Agana *et al.* 2011; Agana *et al.* 2012) that a 50 nm ceramic ultrafiltration membrane can be used to recover wastewater generated at a car manufacturer's post-electrodeposition rinsing stage. Likewise, Anderson *et al.* (1981) have shown that a cellulose acetate RO membrane can work successfully in reclaiming wastewater generated from an automotive electrocoat painting process. In terms of beverage production, Tay and Jeyaseelan (1995) have demonstrated the viability of a combined UF and RO treatment system in the reclamation of bottle-washing wastewater. They concluded that the combined UF and RO system not only reduces freshwater consumption but also conserves energy.

Membranes have also been shown to work successfully in treating similar wastewater streams generated by different production facilities. For example, in an experiment involving the treatment of vegetable oil-contaminated factory wastewater, using a polysulfone UF membrane (Mohammadi & Esmaeilifar 2004), reductions in water quality parameters such as COD, TOC, TSS, and phosphate concentration exceeded 85 %. Similarly, good retention rates for emulsified solvent and oil and grease were obtained when a cellulose acetate UF membrane was used for treatment of spent solvent rinses from nickel-plating operations (Qin *et al.* 2004). The retention rates for emulsified solvent and oil and grease were reported to be 96 % and 80 % respectively.

Although a number of investigations have been carried out with respect to the membrane treatment of wastewater generated by car manufacturing and beverage production processes individually, to the best of our knowledge, no work has carried out that compares the suitability of identified membranes in reclaiming wastewater generated by these contrasting large industries.

The work described in this paper was aimed at determining the suitability of selected polymeric membranes (UF, NF and RO) for the reclamation of wastewater generated at the production facilities of a car manufacturer and a beverage producer. Wastewater streams generated at both of these two production facilities have substantial volumes – making wastewater reclamation desirable in order to reduce excessive water consumption. The suitability of the selected membranes was evaluated based on reduction/rejection rates in relation to critical water quality parameters, permeate flux decline rates and power usage. Likewise, to visualize the degree of fouling on the membrane surface, fouled membranes were analysed using a field emission scanning electron microscope (FESEM). In general, the UF membranes were evaluated for pretreatment of wastewater whilst the NF and RO membranes were evaluated for wastewater reclamation.

METHODS

Wastewater samples

Actual wastewater samples were obtained from a car manufacturer and a beverage producer operating in the western suburbs of Melbourne, Australia. The samples were collected in 20 L containers and kept in a cold room at a temperature of 4 °C. Prior to

every experiment, a specified sample volume is transferred into a stainless steel container. The container is then left for a couple of hours inside the laboratory to bring up the wastewater temperature to ambient level. All samples were used within 48 hours of collection.

UF membranes

Two types of polymeric flat sheet UF membranes, supplied by GE Osmonics, were used in the experiments – namely, JW (polyvinylidene-difluoride, PVDF) membrane with MWCO of 30 kD (pore size = 3.25 nm) and MW (polyacrylonitrile, PAN) membrane with MWCO of 100 kD (pore size = 10 nm). The JW membrane is hydrophobic (contact angle = 66°) while the MW membrane is extremely hydrophilic (contact angle = 4°). UF membranes used for experiments were soaked in deionized water overnight to remove any surface impurities.

NF and RO membranes

Both the NF (DL series) and low-pressure RO (AK series) membranes used in the experiments were supplied by GE Osmonics. The NF membrane is a thin-film membrane having an approximate MWCO of 0.15 – 0.30 kD for uncharged organic molecules. Similar to the NF membrane, the RO membrane is also a thin-film membrane having high flux and a NaCl rejection rate of approximately 99.0 %. The NF membrane was specifically tested on the metals wastewater sample while the RO membrane was tested on all the wastewater samples.

NF and RO membranes preparation

All NF and RO membranes used in the experiments were soaked in deionized water overnight to remove any surface impurities. Prior to using the NF and RO membranes, a wetting protocol was followed (Jezowska *et al.* 2006; Mänttari *et al.* 2002). In this case, deionized water having an average conductivity of 2 µS/cm was pumped into the membrane for 15 minutes. The pressure and temperature of the deionized water was maintained at 2.5 MPa and 25 °C respectively throughout the wetting period.

Membrane filtration system

A schematic diagram of the membrane filtration system used in the experiments is shown in Figure 1. A variable speed pump with ½ hp motor was used to deliver wastewater into the flat sheet test cell (Sterlitech CF 042 Development Cell). Membrane permeate was collected into a container and weighed while reject water was returned into the feed tank to facilitate increase of feed water concentration and fast track the rate of membrane fouling. The feed tank was submerged halfway into a water bath to maintain the temperature within a specified range. Operating parameters such as power usage, pressures, temperatures, weights, and water qualities (pH and conductivity) were monitored at set intervals using probes and recorders connected to a computer.

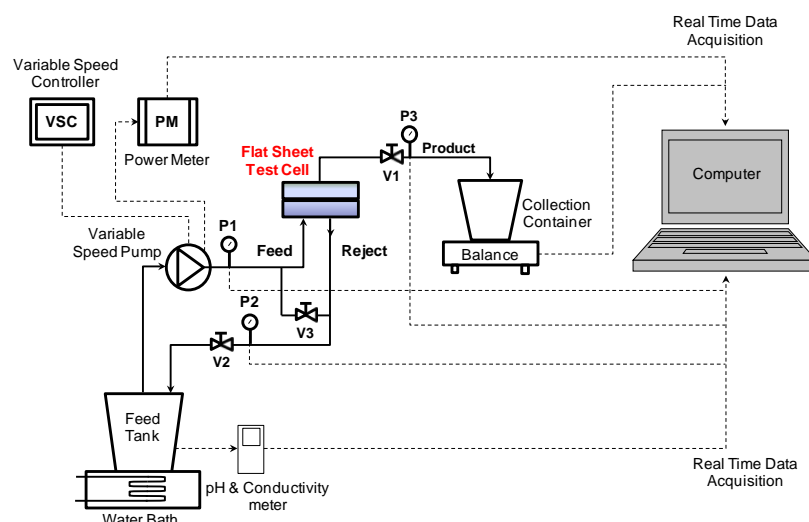


Figure 1 Schematic diagram of the laboratory-scale membrane filtration system used in the experiments. P – pressure gauge; V – valve. Solid lines represent water flow while broken lines represent real time data acquisition.

UF experiments

Wastewater samples collected were directly used as feed into the UF membranes. Experiments were carried out at a crossflow velocity (CFV) of 2.4 m s^{-1} and at transmembrane pressures (TMPs) of 0.2 and 0.4 MPa. The temperature range during the experiments was maintained within $19 - 24 \text{ }^{\circ}\text{C}$. Operating parameters previously mentioned were continuously monitored at 15 minute intervals. Samples of feedwater and membrane permeate were collected into containers and sent to a NATA (National Association of Testing Authorities) accredited laboratory for analysis on water quality parameters such as oil & grease (O&G) and total organic carbon (TOC). Aside from O&G and TOC, feedwater and membrane permeate turbidity were also measured during the experiments to estimate suspended particle rejection rates. The volume of wastewater sample used for each experiment is 6 L while filtration area for all UF membranes used is 0.0042 m^2 . Each experimental run lasted for approximately 6 hrs.

NF and RO experiments

Prior to actual experiments, wastewater samples collected were filtered through a 0.3 micron filter to remove any suspended particles present. Both the NF and RO membrane experiments were carried out at a CFV of 2.7 m s^{-1} and at TMPs of 0.69, 1.03 and 1.38 MPa. The temperature range during the experiments was maintained within $25 - 29 \text{ }^{\circ}\text{C}$. Operating parameters previously mentioned were continuously monitored at 5 minute intervals. Similar to the UF experiments, samples of feedwater and membrane permeate were collected into containers and sent to a NATA accredited laboratory for analysis on water quality parameters such as chemical oxygen demand (COD), conductivity and metals content. The volume of filtered wastewater sample used in each experiment is 3 L while filtration area for both the NF and RO membranes is 0.0042 m^2 . Each experiment run lasted for approximately 2 hrs.

Analytical methods

The size distribution and zeta potential (ζ) of particles in the actual wastewater samples were measured using a Malvern Zetasizer Nano Series (Nano-ZS). Turbidity measurements were carried out using a La Motte 2020 Series Turbidity meter. The reduction/rejection rates (% P_R) of the critical water quality parameters previously mentioned were calculated using Eq. 1:

$$\% P_R = [(P_F - P_P) / P_F] \times 100 \% \quad (1)$$

where P_F is the parameter concentration in the feedwater (mg L^{-1}) and P_P is the parameter concentration in the membrane permeate (mg L^{-1}).

After each experiment, used membranes were washed with deionized water and air dried at ambient temperature. Representative portions of each air dried membranes were cut (approximately 1 cm^2) and mounted on aluminum stubs with carbon tape. They were then coated with a layer of gold and analysed under a FESEM (Philips XL30 FEG).

RESULTS AND DISCUSSION

Pure water flux (PWF)

Experiments aimed at establishing the relationship between pure water flux (PWF) and TMP were carried out prior to commencing actual wastewater experiments. Distilled water having a conductivity of $2 \mu\text{S/cm}$ was used as feed to ensure that no form of fouling will occur during filtration. Results showed that PWFs of the polymeric membranes were highly correlated ($R^2 > 0.99$) with TMP as shown in Figures 2a and b. A high correlation between PWF and TMP is expected since the only resistance present during the experiments is the intrinsic membrane resistance. The slopes of the line shown in Figures 2a and b give the pure water permeabilities (PWP) of the membranes.

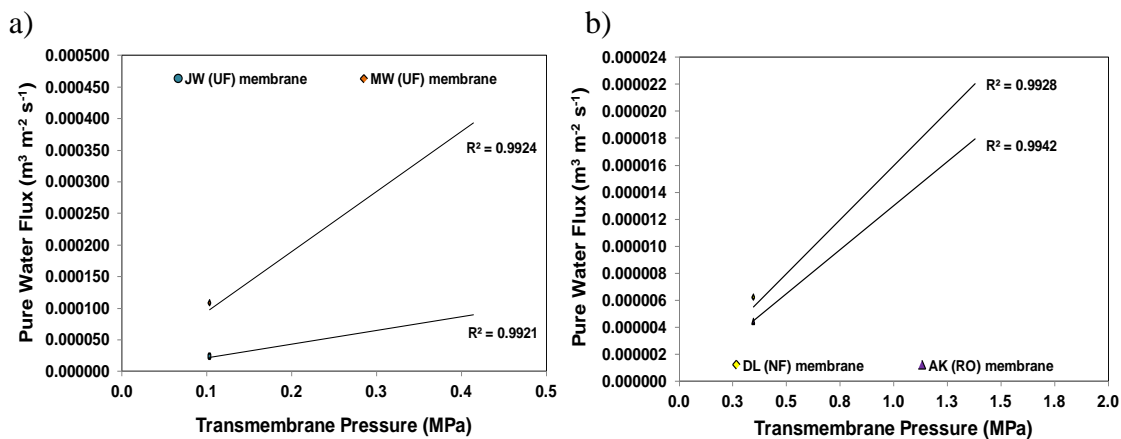


Figure 2 Pure water fluxes of: a) UF membranes as a function of TMP at a CFV of 2.4 m s^{-1} and standard temperature of 20°C and b) NF and RO membranes as a function of TMP at a CFV of 2.7 m s^{-1} and standard temperature of 25°C .

Figure 2a shows that the PWF of the MW membrane was higher than the JW membrane. The disparity between the pure water fluxes of the two UF membranes can be attributed to the relative membrane structure and properties (i.e. hydrophilicity/hydrophobicity). For example, the MW membrane was designed to be extremely hydrophilic and it might be expected to have higher water fluxes than the hydrophobic JW membrane. This scenario is similar to the pure water fluxes obtained for NF and RO membranes (Figure 2b). An NF membrane has relatively looser pores compared to an RO membrane and is expected to have a higher pure water flux.

Characteristics of wastewater samples

The particle size distributions for the wastewater samples collected are shown in Figure 3. The oily and metals wastewater samples obtained from the car manufacturer have particle sizes ranging from 90 – 532 nm and 18 – 397 nm respectively. The mean diameter of the particle sizes found on the oily wastewater sample is 245.5 nm while the mean diameter of particle sizes found on the metals wastewater sample is 134.1 nm. On the other hand, wastewater samples from the beverage producer have particle sizes in the range of 24 to 5560 nm – with a mean diameter of 161.4 nm.

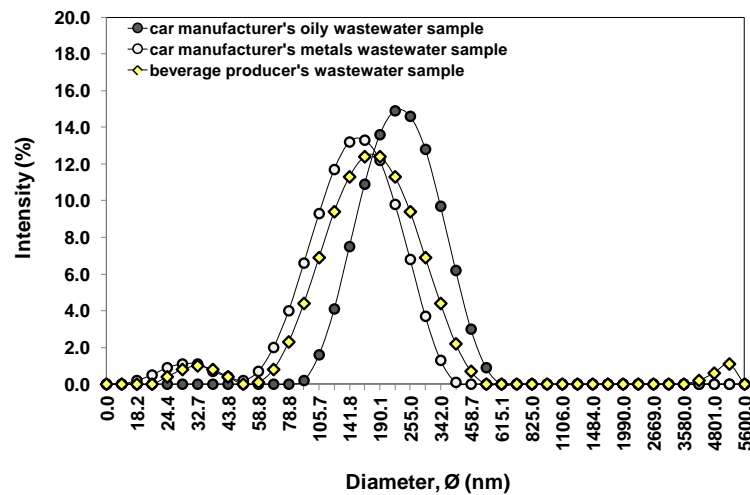


Figure 3 Particle size distributions for wastewater samples used in the experiments.

The average zeta potential (ζ) of the particles present in the wastewater samples collected are shown in Table 1.

Table 1 Average zeta potential (ζ) of particles found on the wastewater samples

Wastewater sample	pH	Particle zeta potential (ζ)
Car manufacturer's oily wastewater sample	7.5	56 ± 2 mV
Car manufacturer's metals wastewater sample	3.8	$- 21 \pm 2$ mV
Beverage producer's wastewater sample	8.3	$- 23 \pm 2$ mV

The values of the zeta potential for both the metals and beverage production wastewater samples suggest that the particles present have incipient instability (ASTM 1985). Because particles present in these wastewater samples are likely to exhibit instability, particle aggregation may occur. Particle aggregation is not considered to be a problem

during ultrafiltration because the more the particles aggregate, the better. Larger particles have higher hydrodynamic forces acting on them and therefore are more likely to be swept away from the membrane surface. In contrast, the zeta potential of particles found in the oily wastewater sample suggests that the particles have good stability and are well dispersed in solution. Since particles are well dispersed in solution, particle aggregation is unlikely to happen. In this particular case, the particle sizes present in the oily wastewater sample can be assumed to be the same throughout the experiments. Therefore, the possibility for the finer suspended particles to deposit on the membrane surface is high.

The typical characteristics of the wastewater samples used in the experiments are shown in Table 2.

Table 2 Typical characteristics of wastewater samples used in the experiments

Water quality parameters	Oily wastewater sample	Metals wastewater sample	Beverage production wastewater sample
pH	7.5	3.8	8.3
Conductivity, $\mu\text{S cm}^{-1}$	979	1579	1129
COD, mg L^{-1}	230	91	4900
O&G, mg L^{-1}	21	<5	17
TOC, mg L^{-1}	120	16	140
Turbidity, NTU	294	43	58
Color	light gray	hazy white	murky, yellowish
Phosphorus, mg L^{-1}	5	71	-
Iron (Fe), mg L^{-1}	1.13	4	-
Manganese (Mn), mg L^{-1}	0.06	23	-
Nickel (Ni), mg L^{-1}	0.02	40	-
Zinc (Zn), mg L^{-1}	1.23	98	-

UF experiments

Permeate fluxes (J , $\text{m}^3 \text{m}^{-2} \text{s}^{-1}$) were calculated using Eq. (2):

$$J = (0.001 \times W) / (A_M \times t) \quad (2)$$

where W is the weight measured by the balance (kg), A_M is the effective membrane area (m^2), t is the sampling time (s). To account for temperature variations, all permeate fluxes were standardized at a temperature of 20 °C using Eq. (3) (Crittenden *et al.* 2005):

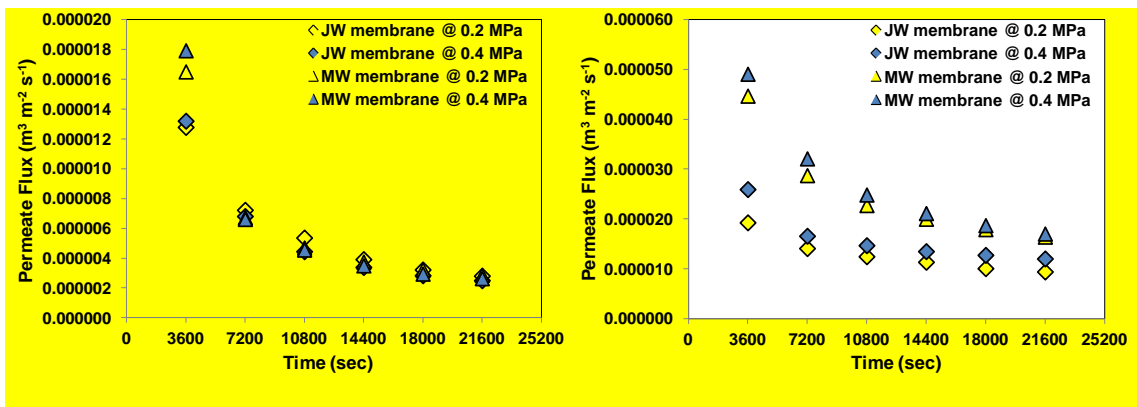
$$J_{20^\circ\text{C}} = J (1.03)^{T_S - T_M} \quad (3)$$

where $J_{20^{\circ}\text{C}}$ is the flux at a standard temperature of 20°C ($\text{m}^3 \text{m}^{-2} \text{s}^{-1}$), T_S is the standard temperature (20°C), T_M is the measured temperature ($^{\circ}\text{C}$).

Both the JW and MW membranes showed the same flux decline profiles when tested on the oily wastewater sample (Figure 4a). A rapid decline in flux was observed after 2 hrs followed by a gradual decline throughout the remainder of the experiment run. Of the two membranes tested for this specific wastewater sample, the MW membrane showed the worst flux decline rates at all TMPs used, which can be explained by considering the membrane's permeability. As noted previously, the pure water permeability of the MW membrane is significantly higher than for the JW membrane (Figure 2a). Howe et al. (2007) showed that membranes with higher permeability fouled faster than membranes with lower permeability. Membranes with higher permeability have bigger pores compared to those with lower permeability. Initially, membranes with bigger pores will have higher fluxes but once particles start to deposit on the pores, fluxes obtained will drastically be reduced until such time that the pore openings have become smaller. Consequently, the smaller pore openings will inhibit further deposition of particles – resulting in gradual flux decline.

a) Oily wastewater sample

b) Metals wastewater sample



c) Beverage production wastewater sample

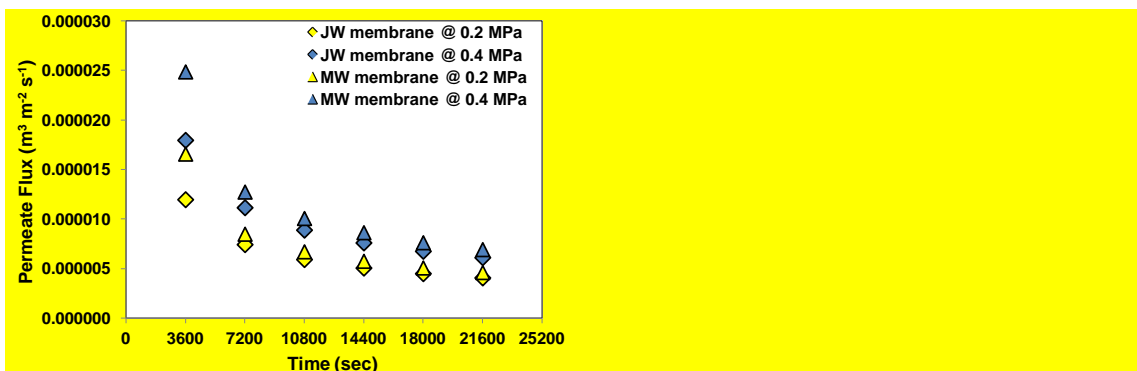


Figure 4 Permeate fluxes obtained for JW and MW membranes.

Fouling rates during the experiments that involved the oily wastewater sample were greatly influenced by the presence of suspended cathodic electrodeposition (CED) paint particles. These particles include paint pigment, unstable resins and polymers. Positively charged cathodic electrodeposition paint particles deposit rapidly on the

surfaces of the JW and MW membranes. The combination of membrane surface-particle interaction and applied transmembrane pressure (TMP) resulted in intense fouling of both membranes. Fouling mechanisms observed during the oily wastewater experiments include intermediate pore blocking and cake layer formation. Intermediate pore blocking occurred during the first two hours of the experiments resulting in rapid flux decline (Figure 4a). Subsequently, cake layer formation was the prevailing fouling mechanism during the remaining experiment time. Deposition of paint particles happen initially on the membrane pores and was followed by accumulation of particles on the membrane surface, resulting in cake layer formation. Fouling of the MW membrane was more severe than for the JW membrane because it has larger pore sizes and higher surface porosity, as shown in Figures 5a and b. Aside from membrane structure, charge attraction can also be a contributing factor in the rapid deposition of CED paint particles on the pores and surface of the MW membrane. Since the CED paint particles are positively charged (Streitberger 2007), they are attracted to the negatively charged surface of the MW membrane. The MW membrane was modified by its manufacturer to become extremely hydrophilic (GE Water and Process Technologies: MW Series Fact Sheet). Such membrane modification usually involves the partial hydrolysis of the membrane material with NaOH – resulting in improved hydrophilicity and a negative surface charge (Wang *et al.* 2007).

The degree of deposition of CED paint particles on the surfaces of the JW and MW membranes are shown in Figures 6a and b. As previously mentioned, surface-particle interaction and applied TMP resulted in intense fouling of the membranes. During the ultrafiltration of the oily wastewater sample, CED paint particles continuously deposit on the membrane surface. The particles that have already deposited on the membrane surface are then compressed leading to higher cake resistance and low permeate flux. The reduction of permeate flux is further magnified at higher TMPs as shown in Figure 4a. Higher pressures cause the cake layer on the membrane surface to compress further resulting in a much lower permeate flux.

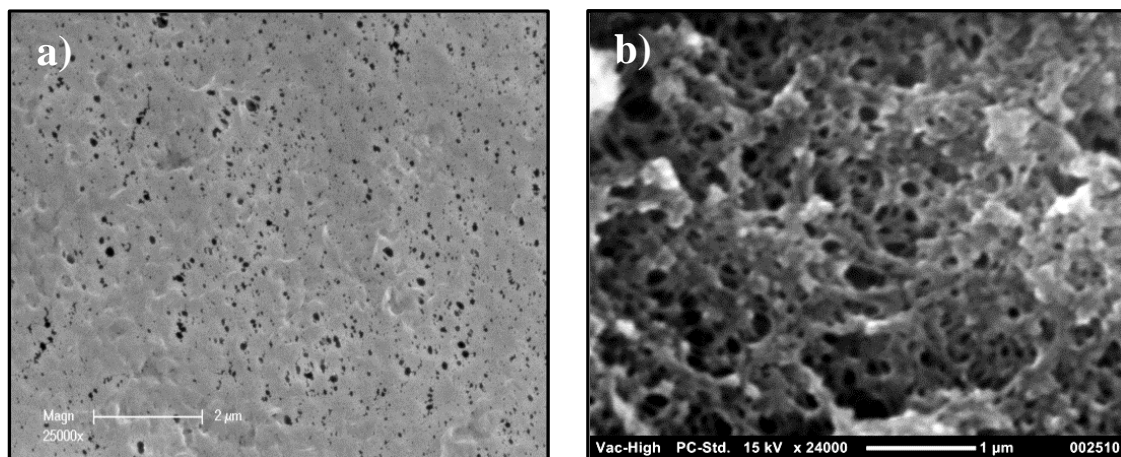


Figure 5 Surface structures of fresh: a) JW and b) MW membranes.

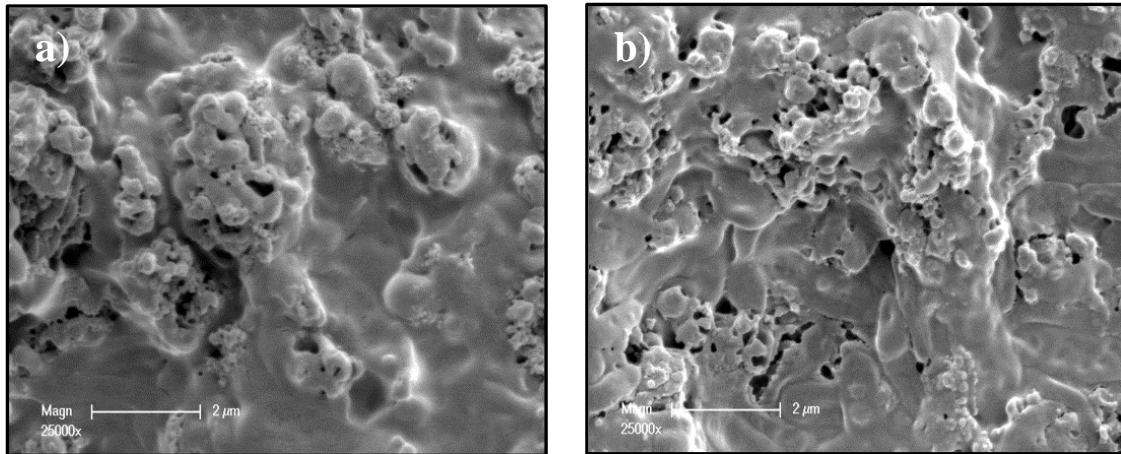


Figure 6 Surface images of a) JW and b) MW membranes used for oily wastewater sample.

For the three different kinds of wastewater stream, the JW and MW membranes performed better for the metals wastewater sample (automobile manufacturer), as shown in Figure 4b – with a relatively higher permeate flux being achieved for both membranes. This was particularly noticeable for the MW membrane which achieved steady-state permeate fluxes of approximately 0.000016 and $0.000017 \text{ m}^3 \text{ m}^{-2} \text{ s}^{-1}$ at TMPs of 0.2 and 0.4 MPa respectively. However, although the MW membrane had higher permeate fluxes, its flux decline rates were relatively higher than for the JW membrane – as shown in Figure 4b. This suggests that a JW membrane may be more suitable for the metals wastewater sample than the MW membrane. The higher flux decline rates experienced by the MW membrane is a sign of intense fouling. A membrane intensely fouled may require longer cleaning time and the use of aggressive chemicals in order to be regenerated. Such scenario may lead to premature membrane material degradation and shorter lifespan.

The relatively improved performance of both membranes for the metals wastewater sample can be attributed to the instability of the particles present in this type of wastewater. As mentioned previously, Table 1, the instability of the suspended particles will promote aggregation. It may be argued that because particles present in the metals wastewater sample have a tendency to aggregate, the cake layers formed on the surfaces of both membranes (Figures 7a and b) were more porous compared to the cake layers formed during experiments involving the oily wastewater sample. Likewise, the dominant fouling mechanism involved during the experiments can be deduced to be cake layer formation.

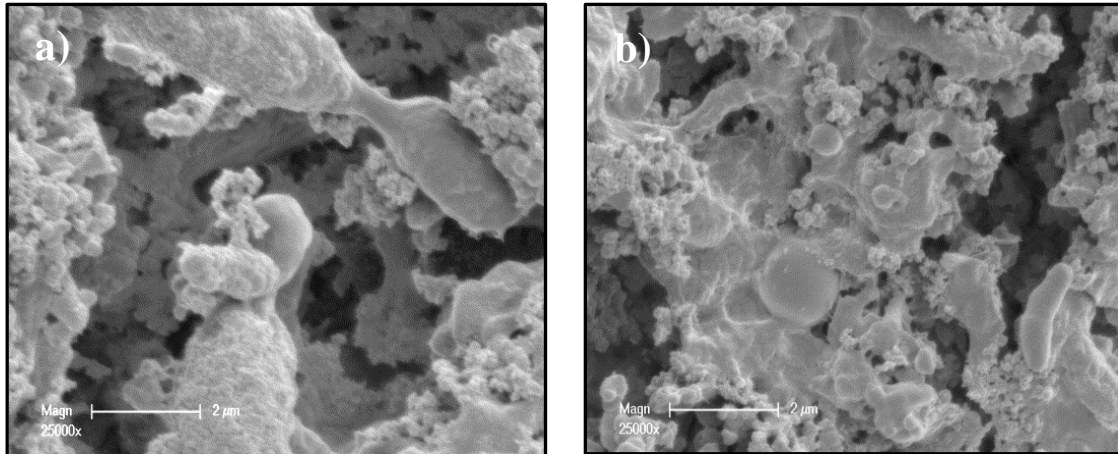


Figure 7 Surface images of a) JW and b) MW membranes used for metals wastewater sample.

Improvement in permeate fluxes for both the JW and MW membranes during experiments involving the beverage production wastewater were not significant as compared to permeate fluxes obtained during experiments on the metals wastewater sample from the automobile manufacturer (Figure 4c). Although the particles present have the tendency to aggregate due to instability, surface-particle interaction and applied TMP negated the effects of hydrodynamic forces on the larger particles formed. Suspended particles commonly made up of dirt and beverage pigments rapidly deposit on the membrane surface. The deposited particles are then continuously compressed resulting in low membrane porosity (Figures 8a and b) and permeate flux. Such a scenario was also observed at a TMP of 0.4 MPa – although permeate fluxes obtained were slightly higher. Of the two UF membranes used, the JW membrane showed slightly lower flux decline rates – as shown in Figure 4c. In general, the fouling mechanisms involved can be deduced as being a combination of intermediate pore blocking and cake layer formation. Deposition of suspended particles happens initially on the membrane pores and was followed by accumulation of particles on the membrane surface.

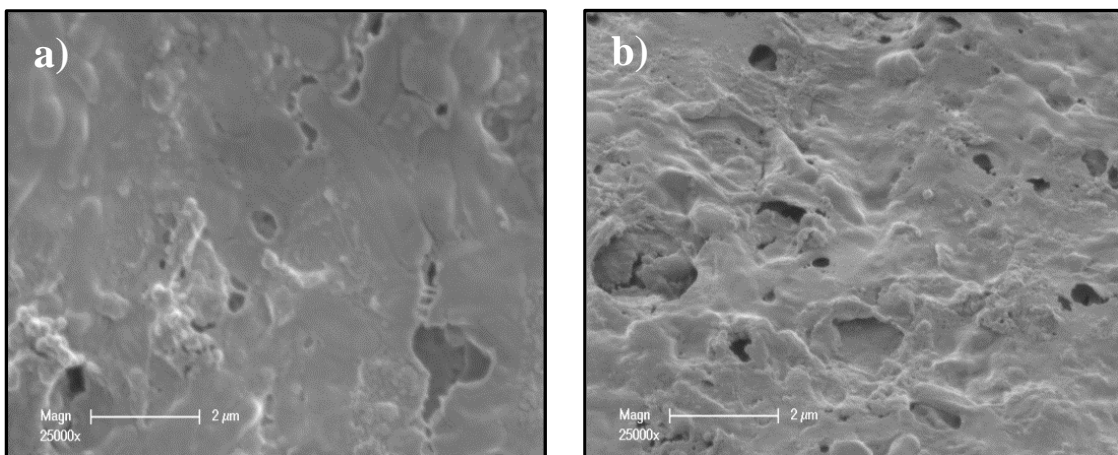


Figure 8 Surface images of a) JW and b) MW membranes used for beverage production wastewater sample.

Turbidity and O&G reduction rates obtained for both the JW and MW membranes show minimal variations– as shown in Figures 9a to c. In general, for all types of wastewater samples used, both membranes achieved turbidity reduction rates of above 98%. Likewise, both membranes also achieved 100% removal of O&G for all wastewater samples used. In terms of TOC reduction, the performance of the two membranes varied with TMP. When evaluated on the oily wastewater sample, the JW membrane's TOC reduction rate appeared to increase with an increase in TMP, while the MW membrane's TOC reduction rate appeared to decrease with an increase in TMP (Figure 9a). Although these experiments were not performed in replicate, such a TOC rejection characteristic, as exhibited by the MW membrane for an oily wastewater sample, is consistent with the results obtained by Akdemir and Ozer (2009). On the other hand, when the membranes were evaluated on the metals and beverage production wastewater samples, TOC reduction rates for both membranes appeared to show a slight increase when the TMP was increased from 0.2 to 0.4 MPa (Figures 9b and c). Notably, the highest TOC reduction for both membranes were obtained from UF experiments involving the beverage production wastewater sample; the TOC reduction rates being above 80% - suggesting that most of the TOC content of the beverage production wastewater may be associated with suspended solids.

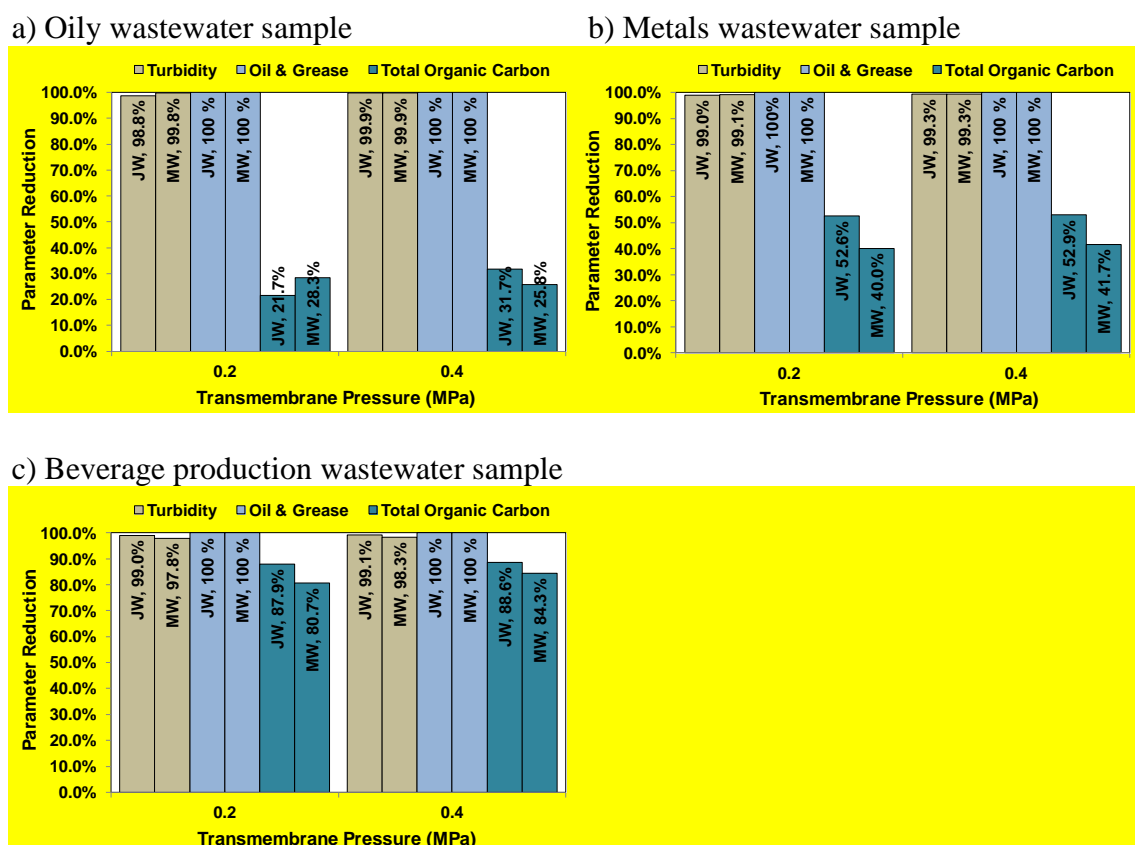


Figure 9 Performance of the JW and MW membranes on the reduction of water quality parameters such as turbidity, O&G and TOC.

NF and RO experiments

Similar to the UF experiments, the permeate fluxes for both the NF and RO membranes were calculated using Eq. (2). To account for temperature variations, all permeate fluxes were standardized at a temperature of 25 °C using Eq. (4):

$$J_{25^{\circ}\text{C}} = J / \text{TCF} \quad (4)$$

where $J_{25^{\circ}\text{C}}$ is the flux at a standard temperature of 25 °C ($\text{m}^3 \text{m}^{-2} \text{s}^{-1}$), J is the actual flux measured ($\text{m}^3 \text{m}^{-2} \text{s}^{-1}$) and TCF is the temperature correction factor (dimensionless). The TCF can be estimated using eq. (5) (Crittenden *et al.* 2005):

$$\text{TCF} = (1.03)^{T_M - 25} \quad (5)$$

where T_M is the measured temperature (°C).

For the three different wastewater types, the permeate fluxes obtained for the RO (AK) membrane at different TMPs are shown in Figures 10a to c. In general, as the TMP is increased, significant improvements in permeate fluxes were measured for all types of wastewater samples used. The highest permeate fluxes were measured for the beverage production wastewater whilst the lowest permeate fluxes were measured for the metals wastewater sample (automobile manufacturer).

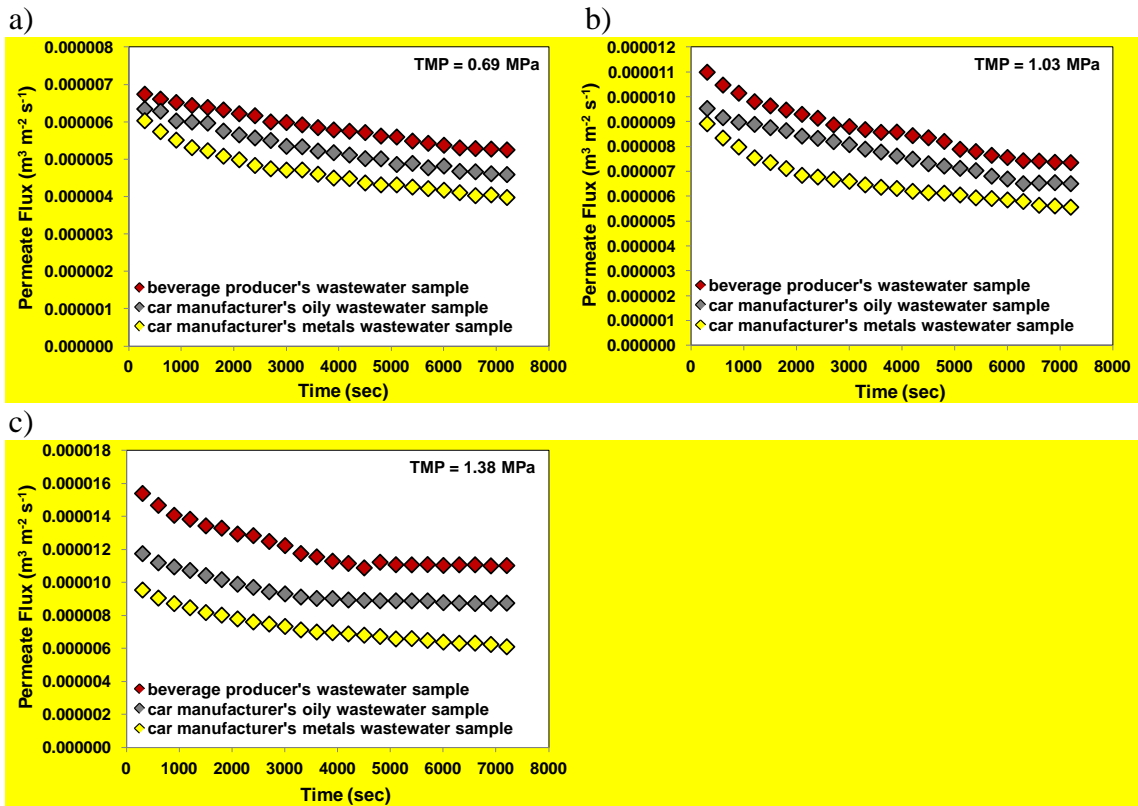


Figure 10 Permeate fluxes obtained for RO (AK) membrane with respect to different wastewater samples used.

It is proposed that the low permeate fluxes obtained for the metals wastewater sample could be due to metal oxide fouling. The metals wastewater sample contains elevated concentrations of heavy metals such as Fe, Mn, Ni, and Zn (Table 2). Iron (Fe), in particular, is known to be susceptible to oxidation (Crittenden *et al.* 2005) and since the apparatus shown in Figure 1 is a closed loop system, the flow of the concentrate back into the feed tank promotes rapid mixing of the wastewater sample. This rapid mixing is similar to aerating a pond to increase dissolved oxygen content. As a result, the process may facilitate the formation of insoluble iron, and other metal oxides, resulting in the deposition of oxide particles onto the surface of the RO membrane (Figures 11b and c). Such fouling would be expected to be further intensified as the pressure increases (Figure 11c).

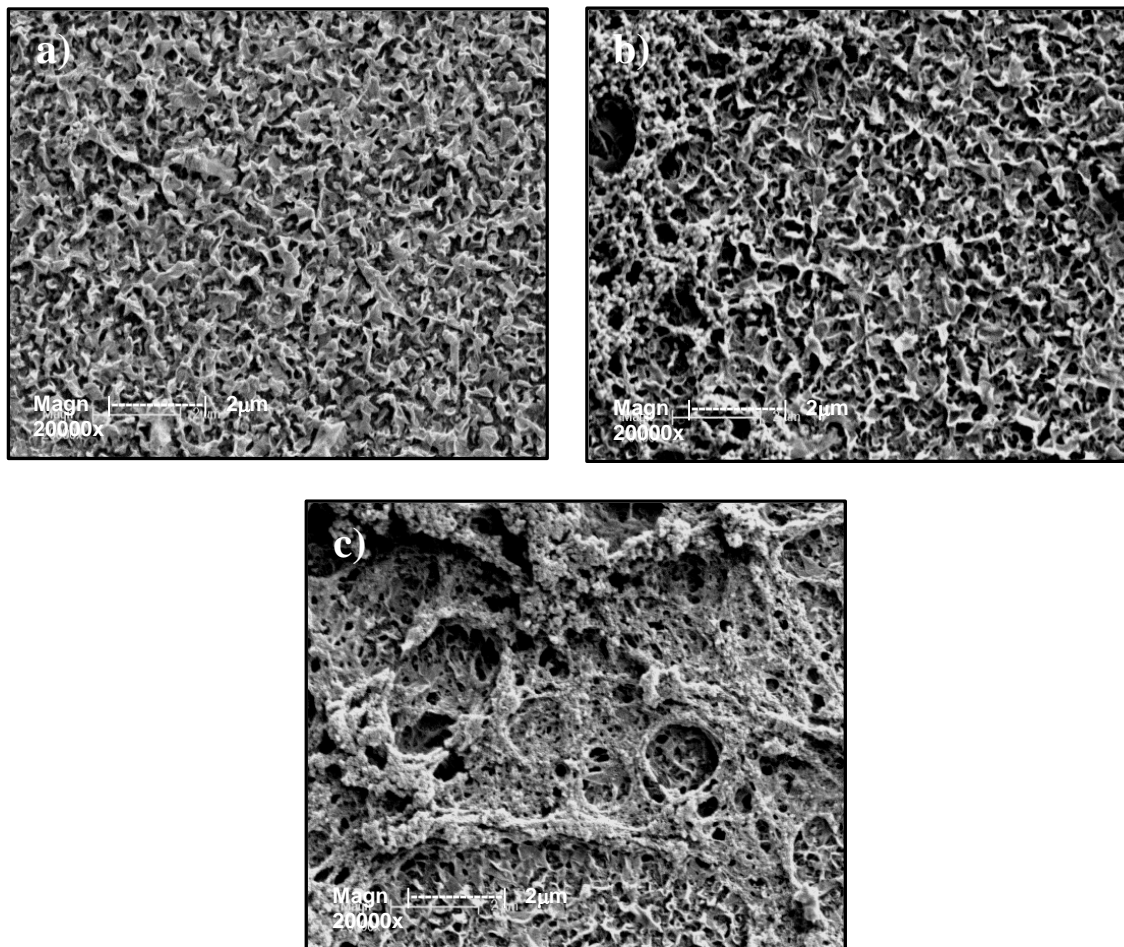


Figure 11 Surface structure of: a) fresh AK membrane, b) AK membrane used for metals wastewater sample at 0.69 MPa and c) AK membrane used for metals wastewater sample at 1.38 MPa.

On the other hand, the highly organic character of the oily and beverage production wastewater samples resulted in relatively higher permeate fluxes for the RO membrane. Such a wastewater characteristic could be considered to suit for the RO membrane given that RO is known to be effective in the separation of organic molecules (Pinnekamp & Friedrich 2006). Because the two wastewater samples mentioned mostly contain organic contaminants, a less severe membrane fouling might be expected, even at a high TMP of 1.38 MPa, and this appears to be evident from the electron

micrographs shown in Figures 12a and b. Aside from higher permeate fluxes, the RO membrane used also had high conductivity and COD reduction rates. With respect to the oily wastewater sample, conductivity and COD reduction rates were more than 96.0% and 98.0% respectively. With respect to the beverage production wastewater sample, conductivity and COD reduction rates were both more than 98.0 %. Conductivity and COD reduction rates for both the beverage production and oily wastewater samples appeared to be dependent on applied TMP – as shown in Figures 13a and b.

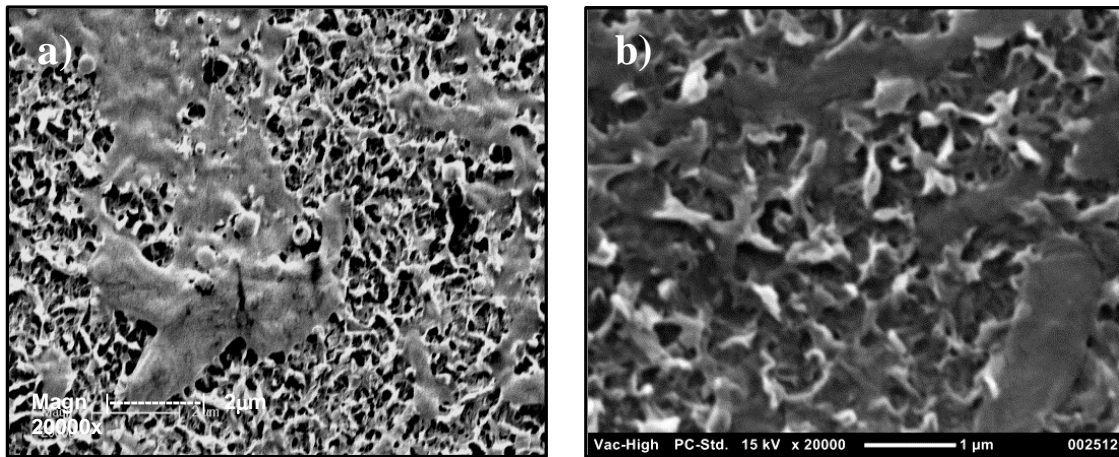


Figure 12 Surface structure of: a) AK membrane used for oily wastewater sample at 1.38 MPa and b) AK membrane used for beverage production wastewater sample at 1.38 MPa.

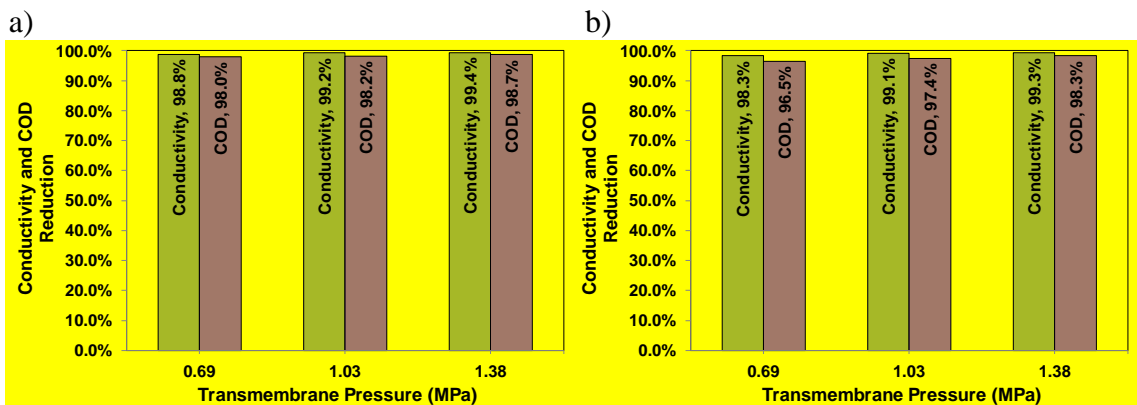


Figure 13 Conductivity and COD reduction rates of RO (AK) membrane with respect to: a) beverage production wastewater sample and b) oily wastewater sample.

An NF (DL series) membrane was also evaluated with respect to the metals wastewater sample since this type of membrane has been reported in literature to be effective in removing heavy metals present in wastewater streams (Ahn *et al.* 1999; Frarès *et al.* 2005; Mohammad *et al.* 2004; Qdais & Moussa 2004). The results of our experiments show that permeate fluxes obtained for the NF membrane were approximately two times higher than the permeate fluxes obtained for the RO membrane, as shown in Figures 14a to c. The superior performance of the NF membrane for the metals wastewater sample can be attributed to its separation mechanism. Unlike an RO membrane, whose primary separation mechanism is solution-diffusion, an NF

membrane combines solution-diffusion and charge repulsion mechanisms to separate dissolved organic molecules and polyvalent inorganic ions (Mohammad *et al.* 2004; Pinnekamp & Friedrich 2006). The inherent charge on the NF membrane's surface would be expected to facilitate the rejection of similarly charged solutes. Likewise, because of this surface charge, it is also able to effectively reject similarly charged metal species (Mohammad *et al.* 2004) and metal oxide particles present in the metals wastewater sample. Consequently, fouling of the NF membrane due to the formation of insoluble metal oxide particles would be expected to be inhibited. Assuming that the observed deposition on the membrane surface is primarily metal oxide, Figures 15b and c demonstrate that, even at high TMP, the material does not appear to be significantly compressed onto the surface.

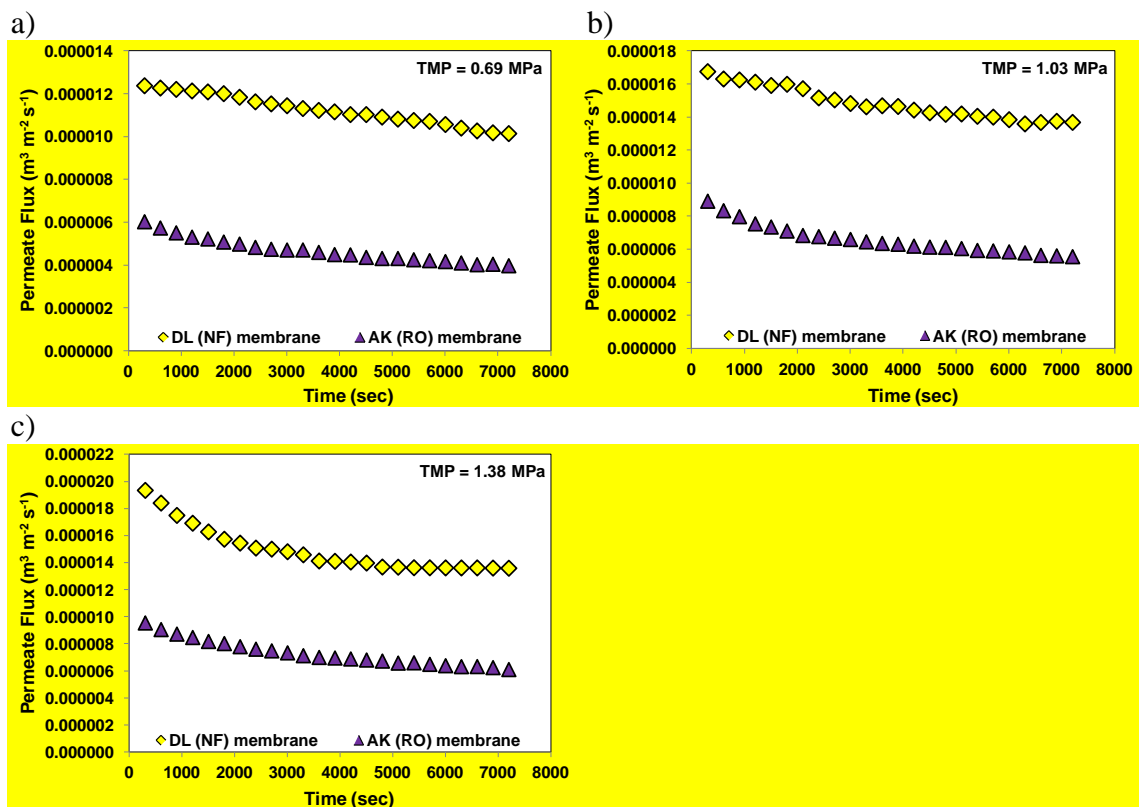
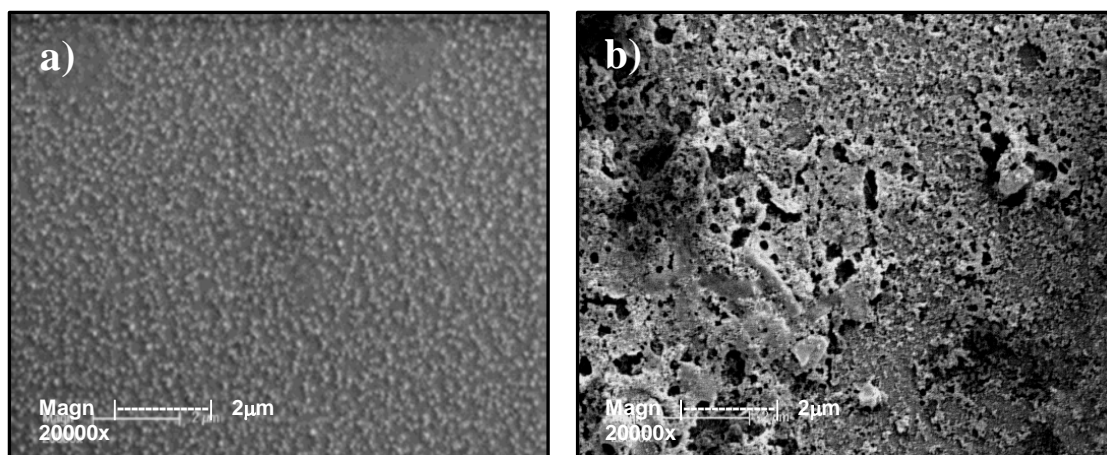


Figure 14 Permeate fluxes measured for RO (AK) and NF (DL) membranes with respect to metals wastewater sample.



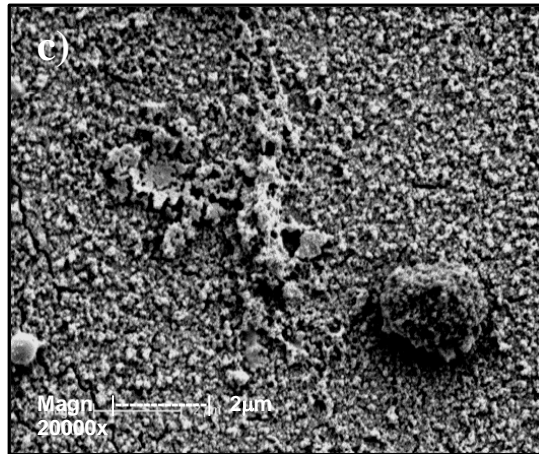


Figure 15 Surface structure of: a) fresh DL membrane, b) DL membrane used for metals wastewater sample at 0.69 MPa and c) DL membrane used for metals wastewater sample at 1.38 MPa.

The conductivity reduction for both the NF (DL) and RO (AK) membranes with respect to the metals wastewater sample show values of more than 60.0 % at all TMPs used (Figure 16a). This suggests that a single pass system is not enough if water reclamation is aimed at replacing citywater to be supplied to processes. In terms of COD reduction, the RO membrane appears to have relatively higher reduction rates than the NF membrane (Figure 16b). For the RO membrane, COD reduction rates were more than 94.0 %, while for the NF membrane, COD reduction was just above 74.0 %. In general, conductivity and COD reduction rates were slightly dependent on TMP – as TMP increased, reduction rates slightly increased.

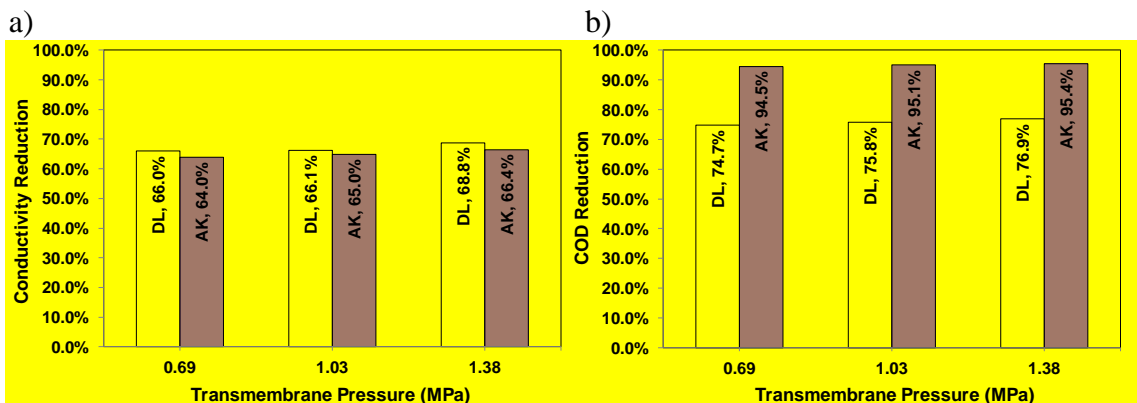


Figure 16 a) Conductivity and b) COD reduction rates of NF (DL) and RO (AK) membranes with respect to metals wastewater sample.

Both NF and RO membranes showed rejection rates of more than 99.0 % for the metals Mn, Ni and Zn. Interestingly, with respect to Fe, the NF membrane had rejection rates of 84.0 %, 86.2 % and 87.5 % while the RO membrane had lower rejection rates – 58.3 %, 59.6 % and 62.2 % (Figures 17a and b). The selective passage of iron through both membranes, although intriguing, has not been investigated further in this study. However, it is tempting to relate this to the fact that the iron is likely to be trivalent whereas the other metals are all divalent. The phenomenon might also be related to the

relative speciation profiles of the different metals in the wastewater. Additionally, the work conducted by Diallo *et al.* (2013) showed that at high acid concentration, chloride retention is negative – suggesting that electrostatic interactions can have an influence in the transfer mechanism during nanofiltration. This result was based on a model solution of iron chloride ($18.6 \times 10^{-3} \text{ mol L}^{-1} \text{ FeCl}_3$) mixed in different concentrations of phosphoric acid (H_3PO_4 : 0.12, 1.2 and 5.9 mol L^{-1}) (Diallo *et al.* 2013).

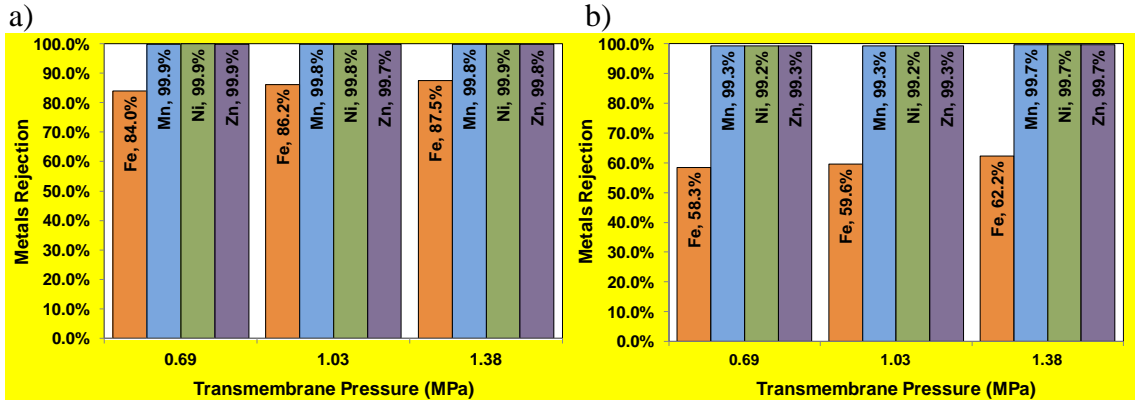


Figure 17 Metals rejection rates of a) NF (DL) and b) RO (AK) membranes with respect to metals wastewater sample.

Energy consumption

In general, improvements in permeate fluxes and reduction/rejection rates of critical water quality parameters were achieved at higher TMPs. However, maintaining higher TMPs usually involve the consumption of substantial amounts of energy, especially for systems requiring larger pumps (Agana *et al.* 2011). To investigate this further at a laboratory-scale level, the average power consumption (P , kW) of the pump motor for each experiment run was recorded. The recorded power consumptions were subsequently used to calculate total energy consumptions (EC_T , kWh) using Eq. (6):

$$EC_T = Pt \quad (6)$$

where t is the experiment duration (hr). Tables 3 and 4 show the energy consumptions of all the membranes used on specific wastewater samples.

For the UF experiments, minimal increase in energy consumption was obtained when TMP was increased from 0.2 to 0.4 MPa (Table 3). On the average, the increase in energy consumption was approximately 2.0 %. On the other hand, a significant increase in energy consumption was calculated for the NF and RO experiments. When TMP was increased from 0.69 to 1.03 MPa, an average increase of approximately 18.0 % was obtained. Increasing the TMP further to 1.38 MPa resulted in an additional average increase of 18.0 %. It is also worth mentioning that the energy consumption of the RO membrane was comparable to the NF membrane during experiments involving the car manufacturer's metals wastewater sample. The low energy consumption of the RO membrane can be attributed to its inherent characteristic of being a low-pressure membrane.

Table 3 Energy consumptions for ultrafiltration experiments

Sample	JW		MW	
	Energy consumption, kWh			
	@ 0.2 MPa	@ 0.4 MPa	@ 0.2 MPa	@ 0.4 MPa
Car manufacturer’s oily wastewater	0.112	0.114	0.112	0.114
Car manufacturer’s metals wastewater	0.110	0.112	0.110	0.112
Beverage producer’s wastewater	0.110	0.114	0.110	0.114

Table 4 Energy consumptions for nanofiltration and reverse osmosis experiments

Sample	DL			AK		
	Energy consumption, kWh					
	@ 0.69 MPa	@ 1.03 MPa	@1.38 MPa	@ 0.69 MPa	@ 1.03 MPa	@1.38 MPa
Car manufacturer's oily wastewater	-	-	-	0.202	0.236	0.276
Car manufacturer's metals wastewater	0.200	0.238	0.286	0.200	0.240	0.280
Beverage producer's wastewater	-	-	-	0.206	0.238	0.278

CONCLUSIONS

The above experiments demonstrated the suitability of selected polymeric membranes for the reclamation of different wastewater streams generated by a car manufacturer and a beverage producer. Based on these results, the following conclusions may be made:

1. Both the JW and MW ultrafiltration membranes cannot be used directly as pretreatment for the oily wastewater stream due to the presence of suspended CED paint particles. Although particle deposition can be minimized by increasing the CFV, membrane cleaning of the deposited CED paint particles is the main problem. The nature and frequency of cleaning to remove the deposited CED paint particles may significantly degrade the membrane material – leading to a shorter membrane lifespan.
2. Of the two ultrafiltration membranes tested on the beverage production wastewater stream, the JW membrane proved more suitable for pretreatment than the MW membrane. Flux decline rates for the JW membrane were lower as compared to the MW membrane. Likewise, for this specific wastewater stream, the JW membrane showed higher reduction rates with respect to critical water parameters such as turbidity and TOC.
3. The JW membrane was also suitable for pretreatment of the metals wastewater stream. It showed lower flux decline rates and higher turbidity and TOC reduction rates – as compared to the MW membrane.

4. The RO (AK) membrane was suitable for use in the reclamation of two wastewater streams – the oily and beverage production wastewaters. Fouling rates of the RO membrane at these two wastewater streams were slow as reflected on the permeate flux decline rates. Furthermore, reduction rates of critical water quality parameters such as conductivity and COD were high.

5. The NF (DL) membrane was more suitable than the RO (AK) membrane for the reclamation of the metals wastewater stream. Permeate fluxes obtained for the NF membrane at all TMPs used was significantly higher compared to the RO membrane. In terms of metals rejection, the NF membrane generally had higher metals rejection rates than the RO membrane. Although the NF membrane had relatively higher permeate fluxes, its conductivity and COD reduction rates were just above 66.0 and 74.0% respectively. Therefore, the use of a single pass system is not sufficient if reclaimed water is intended for processes requiring Citywater quality (water supplied by local water retailer).

6. Not unexpectedly, the energy consumptions for all the membranes used were dependent on TMP – as TMP is increased, energy consumption also increased. It was found that energy consumption of the RO membrane was comparable to the energy consumption of the NF membrane. The slightly lower energy consumption of the RO membrane can be attributed to its inherent characteristic of being a low-pressure membrane.

REFERENCES

- Agana BA, Reeve D, Orbell JD (2011) Optimization of the operational parameters for a 50 nm ZrO₂ ceramic membrane as applied to the ultrafiltration of post-electrodeposition rinse wastewater. *Desalination*, 278 (1-3), 325-332.
- Agana BA, Reeve D, Orbell JD (2012) The influence of an applied electric field during ceramic ultrafiltration of post-electrodeposition rinse wastewater. *Water Res*, 46 (11), 3574-3584.
- Ahn KH, Song KG, Cha HY, Yeom IT (1999) Removal of ions in nickel electroplating rinse water using low-pressure nanofiltration. *Desalination*, 122 (1), 77-84.
- Akdemir EO, Ozer A (2009) Investigation of two ultrafiltration membranes for treatment of olive oil mill wastewater. *Desalination*, 249 (2), 660-666.
- Anderson JE, Springer WS, Strossberg GG (1981) Application of reverse osmosis to automotive electrocoat paint wastewater recycling. *Desalination*, 36 (2), 179-188.
- ASTM (1985) Zeta Potential of Colloids in Water and Waste Water. ASTM Standard D 4187-82.
- Crittenden JC, Trussell RR, Hand DW, Howe KJ, Tchobanoglous G (2005) Water treatment: Principles and design. 2nd edn. John Wiley & Sons, Inc., Hoboken, NJ.
- Diallo H, Rabiller-Baudry M, Khaless K, Chaufer B (2013) On the electrostatic interactions in the transfer mechanisms of iron during nanofiltration in high concentrated phosphoric acid. *J Membr Sci*, 427, 37-47.
- Frarès NB, Taha S, Dorange G (2005) Influence of the operating conditions on the elimination of zinc ions by nanofiltration. *Desalination*, 185 (1-3), 245-253.

- GE Water and Process Technologies: MW Series Fact Sheet.
http://www.gewater.com/pdf/Fact%20Sheets_Cust/Americas/English/AM-FSpwMWSeries_EN.pdf. Accessed 16/12/11
- Howe KJ, Marwah A, Chiu K-P, Adham SS (2007) Effect of membrane configuration on bench-scale MF and UF fouling experiments. *Water Res*, 41 (17), 3842-3849.
- Jezowska A, Schipolowski T, Wozny G (2006) Influence of simple pre-treatment methods on properties of membrane material. *Desalination*, 189 (1-3 SPEC. ISS.), 43-52.
- Mänttari M, Pihlajamäki A, Kaipainen E, Nyström M (2002) Effect of temperature and membrane pre-treatment by pressure on the filtration properties of nanofiltration membranes. *Desalination*, 145 (1-3), 81-86.
- Mohammad AW, Othaman R, Hilal N (2004) Potential use of nanofiltration membranes in treatment of industrial wastewater from Ni-P electroless plating. *Desalination*, 168 (1-3), 241-252.
- Mohammadi T, Esmaeilifar A (2004) Wastewater treatment using ultrafiltration at a vegetable oil factory. *Desalination*, 166, 329-337.
- Pinnekamp J, Friedrich H (eds) (2006) Municipal Water and Waste Management : Membrane Technology for Waste Water Treatment, vol 2. 2nd edn. FiW VERLAG, Aachen.
- Qdais HA, Moussa H (2004) Removal of heavy metals from wastewater by membrane processes: A comparative study. *Desalination*, 164 (2), 105-110.
- Qin J-J, Wong F-S, Li Y-Q, Nyunt Wai M, Lian Y-T (2004) The use of ultrafiltration for treatment of spent solventcleaning rinses from nickel-plating operations: membrane material selection study. *Desalination*, 170 (2), 169-175.
- Streitberger H (2007) Electrodeposition coatings. In: Streitberger H, Dossel K (eds) Automotive paints and coatings. 2nd edn. Wiley-VCH, Weinheim, pp 89-127
- Tay J-H, Jeyaseelan S (1995) Membrane filtration for reuse of wastewater from beverage industry. *Resour Conserv Recy*, 15 (1), 33-40.
- Wang ZG, Wan LS, Xu ZK (2007) Surface engineerings of polyacrylonitrile-based asymmetric membranes towards biomedical applications: An overview. *J Membr Sci*, 304 (1-2), 8-23.